9-1-2021

Bioactive in situ crosslinkable polymer-peptide hydrogel for cell delivery to the intervertebral disc in a rat model

Marcos N Barcellona
Washington University in St. Louis

Julie E Speer
Washington University in St. Louis

Liufang Jing
Washington University in St. Louis

Deepanjali S Patil
Washington University in St. Louis

Munish C Gupta
Washington University School of Medicine in St. Louis

See next page for additional authors

Acta Biomaterialia 131 (2021) 117–127

Contents lists available at ScienceDirect

Acta Biomaterialia

journal homepage: www.elsevier.com/locate/actbio

Full length article

Bioactive *in situ* crosslinkable polymer-peptide hydrogel for cell delivery to the intervertebral disc in a rat model

Marcos N. Barcellona[a], Julie E. Speer[a], Liufang Jing[a], Deepanjali S. Patil[a], Munish C. Gupta[b], Jacob M. Buchowski[b], Lori A. Setton[a,b,*]

[a] Department of Biomedical Engineering, Washington University in St. Louis, United States
[b] Department of Orthopedic Surgery, Washington University School of Medicine, United States

ARTICLE INFO

Article history:
Received 10 February 2021
Revised 29 June 2021
Accepted 29 June 2021
Available online 4 July 2021

Keywords:
Nucleus pulposus
3D cell culture
Cell adhesive mimetic peptide
In vivo

ABSTRACT

Degeneration of the intervertebral disc (IVD) is associated with significant biochemical and morphological changes that include a loss of disc height, decreased water content and decreased cellularity. Cell delivery has been widely explored as a strategy to supplement the nucleus pulposus (NP) region of the degenerated IVD in both pre-clinical and clinical trials, using progenitor or primary cell sources. We previously demonstrated an ability for a polymer-peptide hydrogel, serving as a culture substrate, to promote adult NP cells to undergo a shift from a degenerative fibroblast-like state to a juvenile-like NP phenotype. In the current study, we evaluate the ability for this peptide-functionalized hydrogel to serve as a bioactive system for cell delivery, retention and preservation of a biosynthetic phenotype for primary IVD cells delivered to the rat caudal disc in an anular puncture degeneration model. Our data suggest that encapsulation of adult degenerative human NP cells in a stiff formulation of the hydrogel functionalized with laminin-mimetic peptides IKVAV and AG73 can promote cell viability and increased biosynthetic activity for this population in 3D culture *in vitro*. Delivery of the peptide-functionalized biomaterial with primary rat cells to the degenerated IVD supported NP cell retention and NP-specific protein expression *in vivo*, and promoted improved disc height index (DHI) values and endplate organization compared to untreated degenerated controls. The results of this study suggest the physical cues of this peptide-functionalized hydrogel can serve as a supportive carrier for cell delivery to the IVD.

Statement of significance

Cell delivery into the degenerative intervertebral disc has been widely explored as a strategy to supplement the nucleus pulposus. The current work seeks to employ a biomaterial functionalized with laminin-mimetic peptides as a cell delivery scaffold in order to improve cell retention rates within the intradiscal space, while providing the delivered cells with biomimetic cues in order to promote phenotypic expression and increase biosynthetic activity. The use of the *in situ* crosslinkable material integrated with the native IVD, presenting a system with adequate physical properties to support a degenerative disc.

1. Introduction

The nucleus pulposus (NP) of the intervertebral disc (IVD) has been observed to undergo significant biological, physical, and biochemical changes with ageing, maturation, injury and disease [1–7]. As disc degeneration progresses, changes in matrix composition and tissue cellularity have been reported [6,8–12]. Loss of glycosaminoglycans, changes in extracellular matrix composition, and altered biosynthetic activity all play a role in tissue degeneration, often leading to structural issues at longer length scales such as disc dehydration, tissue stiffening, loss of disc height, and ultimately altered tissue biomechanics [2,3,13–15].

Because the disc has inherently little capacity for self-repair due to low vascularization and nutrient supply, and more importantly

* Corresponding author at: Department of Biomedical Engineering, Washington University in St. Louis, United States.
E-mail address: setton@wustl.edu (L.A. Setton).

https://doi.org/10.1016/j.actbio.2021.06.045

the low native cell density found within the NP, various strategies have been investigated towards the goal of disc height restoration through NP supplementation [16–23]. A number of acellular materials-based approaches have been developed with the goal of providing mechanical support to the spine and/or stimulating the resident NP cells to alter protein expression and biosynthetic activity [16,24–26]. Although these strategies are attractive due to the lack of a cellular component, acellular techniques rely on an interaction between the residing NP cells and the hydrogel for promoting tissue integration and biosynthetic activity [24]. This may be problematic due to the relatively low cell density of the NP [4,23]. Alternatively, cell delivery approaches seek to treat degeneration by supplying an active cell population into the intradiscal space [27–29]. While effective at promoting an increase in biosynthetic activity, cells delivered without a carrier may be short-lived within the disc space, with studies suggesting that carrier-free cell delivery can lead to as much as 90% of the delivered cells leaking out of the disc [27,28,30–32]. It is further useful that the cells be delivered into the disc in a carrier that is able to provide biological and environmental cues that support cell viability and retention of IVD cell phenotypes. Biomaterials of low stiffness (<1 kPa) have been previously demonstrated to support greater biosynthesis and maintenance of the NP-specific cell phenotype [8,33,34] for primary NP cells in culture, giving evidence of an ability for environmental cues such as physical stiffness to regulate NP cell phenotype. However, biomaterials serving as cell carriers should be of sufficient stiffness that they prevent cell motility and integrate with the native tissue, with some potential to contribute mechanical support to the disc. Non-optimal carriers may enable cell leakage from the carrier or induce the cells towards other phenotypes which could either limit the regenerative process, or else, contribute to the degenerative cascade [35]. A desirable strategy for cell-supplemented materials is to promote re-cellularization of the NP while enabling an ability to present bioactive and environmental factors that can promote cell viability, metabolism and synthesis of extracellular matrix [26,36].

A number of studies have used biomaterials with adhesive domains such as collagen or hyaluronan for cell delivery into the IVD [26,37,38]. However, only few studies – as little as 5% of the modified biomaterials reported in the literature – have demonstrated a significant biological effect associated with specific cell-adhesive motifs [39]. The use of biomaterials capable of eliciting biological changes due to peptide-functionalization, in addition to enabling cell delivery and promoting cell retention, may provide translationally meaningful outcomes in the treatment of disc degeneration. In previous work, we developed a peptide-functionalized poly(ethylene glycol) (PEG)-based hydrogel system functionalized with the laminin-mimetic peptides AG73 and IKVAV [40]. We engineered a hydrogel formulation to be of similar stiffness to the degenerative NP (15% PEG w/v, ~10 kPa) and had it benchmarked against a soft hydrogel functionalized with full length laminin-111 protein (4% PEG w/v, ~500 Pa) that has been shown to provide environmental and biological cues supportive of increasing NP cell biosynthesis and maintenance of NP-specific markers [33,34,40,41]. For studies of adult degenerative NP cells cultured in 2D, our data suggested that peptide density could be controlled in order to inhibit focal adhesion formation and regulate cell morphology, promoting desirable degrees of bioactivity, gene expression, and protein deposition that emulate the Behavior of cells cultured atop the soft, full-length-laminin functionalized hydrogel [8,34,40]. In the present study, we sought to examine the potential for the stiff PEG hydrogel system, functionalized with laminin-mimetic peptides at lower density, to be used as a 3D system for encapsulation and culture of human adult degenerative IVD cells *in vitro*. We further evaluate the ability of this platform to restore parameters of the non-degenerative IVD following injectable delivery of encapsulated primary NP cells into rat caudal discs following degeneration induced via a surgical puncture model [29,42–47]. The results suggest that the stiff, low-peptide density functionalized hydrogel promoted bioactivity and matrix synthesis similar to that of a soft PEG hydrogel functionalized with full-length laminin for human IVD cells encapsulated in 3D during *in vitro* culture. Primary rat IVD cells delivered to the discs via the peptide-functionalized hydrogel remained viable for 8-weeks following injection and demonstrated deposition of new matrix and expression of NP-specific protein biomarkers. Furthermore, implantation of the cell-laden peptide-functionalized hydrogels into the degenerative disc space demonstrated improvements in disc height indices and degeneration-induced alterations to the endplates as compared to untreated controls.

2. Methods

2.1. NP cell isolation

For *in vitro* cell culture experiments, primary adult human NP cells (33 y/o male, 49 y/o female, 30 y/o male, and 68 y/o female) were isolated as previously described [40,48]. Briefly, to-be-discarded tissue from patients undergoing surgical treatment for degenerative spine conditions was collected, and age and sex information was gathered for experimental purposes; grade of pathology and vertebral level remained unknown. For cell isolation, NP tissue was identified and placed for 2–4 h at 37 °C and 5% CO_2 in digestion medium containing 0.4% type 2 collagenase (Worthington Biochemical, Lakewood, NK) and 0.2% pronase (Roche, Basel, Switzerland). Following, the digestion medium was centrifuged for 10 min at 400 rcf to pellet the cells, and the medium was aspirated. Cells were resuspended in PBS and then passed through a 70 μm filter. The flowthrough was again centrifuged for 10 min at 400 rcf, and the resulting cell pellet was resuspended in Ham's F12 medium (Thermo Fisher Scientific, Waltham, MA), supplemented with 10% foetal bovine serum (FBS) and 1% penicillin-streptomycin (P/S) and cultured in monolayer. Cells were used up to passage 4, as little effect in cell phenotype has been characterized in cells up to this passage number [49].

For *in vivo* studies of NP cell delivery to the intradiscal space, rat NP cells were harvested from caudal discs of male Sprague-Dawley rats (16–20 weeks old, $n = 8$). In brief, spines were isolated immediately following sacrifice. Discs were bisected using a size 11 surgical blade, and the NP tissue was extracted. Rat NP cells were then isolated by placing the tissue in digestion medium containing 0.2% type 2 collagenase (Worthington Biochemical, Lakewood, NK) and 0.3% pronase (Roche) for 2–4 h at 37 °C and 5% CO_2. The digestion medium was similarly washed and filtered as described above. Isolated cells were resuspended in Ham's F12 medium (Thermo Fisher Scientific), supplemented with 10% foetal bovine serum (FBS) and 1% penicillin-streptomycin (P/S) and cultured in monolayer. Rat NP cells were used between passages 1 and 4.

2.2. Hydrogel preparation and in vitro 3D NP cell culture

Maleimide terminated 8-arm star poly(ethylene glycol) (PEG-8MAL, MW 20 K, Creative PEGWorks, Durham, NC) was first dissolved in Ham's F12 cell culture media supplemented with 1% P/S. Lyophilized, cysteine terminated IKVAV and AG73 peptides (full sequences for IKVAV and AG73: CSRARKQAASIKVAVSADR, and CGGRKRLQVQLSIRT respectively, GenScript, Piscataway, NJ) were likewise dissolved in F12 + 1% P/S. A maleimide-thiol Michael-type addition reaction was employed both for peptide conjugation and hydrogel formation [50,51]. Peptide solution was added to the PEG-8MAL at either 100 or 400 μM total peptide using

equimolar amounts of IKVAV and AG73 in order to couple peptides to the PEG-8MAL backbone. A small PEG-dithiol (SH-PEG-SH, MW 600, Creative PEGWorks) crosslinker was dissolved in F12 + 20% FBS + 1% P/S. Primary degenerative adult human NP cells were then suspended in the PEG-dithiol solution at a density of 2.5×10^6 cell/mL. The cell-containing di-thiol crosslinker mix was immediately added to the peptide-functionalized maleimide in wells of a round-bottom 96 well plate to initiate hydrogel formation. Soft PEG-LM constructs were similarly fabricated following previously established protocols [33,52]. Briefly, full-length laminin-111 (LM111, Trevigen, Gaithersburg, MD) was first PEGylated with acrylate-PEG-N-hydroxysuccinimide (Ac-PEG-NHS, MW 10 kDa, CreativePEGWorks, Winston Salem, NC), dialyzed against 0.1 M sodium bicarbonate buffer, and diluted to 2 mg/mL. The PEGylated laminin was then added to PEG-8Ac (4% PEG w/v), and a small PEG-dithiol (SH-PEG-SH, MW 600) crosslinker was added to promote hydrogel formation [33]. Constructs were cultured at 37 °C and 5% CO_2 for 4 days.

2.3. Cell viability, biosynthetic activity, and matrix deposition

Following 3D *in vitro* cell culture of NP, cell viability was surveyed using a live/dead cell viability kit following manufacturer's protocol (Invitrogen, Carlsbad, CA). To assay biosynthetic activity and matrix deposition, a functional noncanonical amino-acid tagging approach was employed [53,54]. Briefly, 3D cell-containing hydrogels were made as described above and cultured in L-methionine free DMEM (Gibco, ThermoFisher, Waltham, MA) supplemented with 100 μM L-azidohomoalanine (AHA, ClickChemistryTools, Scottsdale, AZ). Cell-gel constructs were cultured for 4 days at 37 °C and 5% CO_2. After 4 days, the media was replaced with L-methionine free DMEM supplemented with 30 μM of the AHA-binding secondary DBCO-488 (ClickChemistryTools), and incubated for 45 min at 37 °C and 5% CO_2. The constructs were then washed with PBS 3 times and fixed for 12 min using 4% paraformaldehyde (PFA). Following, cells were stained with Alexa-conjugated phalloidin 633 (1:250, Invitrogen) to visualize cell bodies, and counterstained with DAPI (2 μg/mL, Sigma-Aldrich, St. Louis, MO) to visualize nuclei. Overlaying the phalloidin channel with the AHA channel allowed for the measurement of intracellular AHA presence, which was used as a measure of biosynthetic activity. Five independent ROIs were outlined for each patient, and cells were visualized via confocal microscopy (SPE DM6, Leica Microsystems Buffalo Grove, IL). Extracellular AHA presence was used as a measure of matrix deposition and was calculated as $\frac{Volume_{Matrix}-Volume_{Cell}}{Volume_{Cell}}$, with volumes being calculated from 3D reconstructions of z-stacks using a voxel counter plugin for Fiji. Actin fiber alignment was quantified using the OrientationJ plugin in Fiji, where an output of one indicates strong fiber alignment, and an output of zero indicates anisotropic fiber orientation.

2.4. Immunocytochemistry

3D cell-laden hydrogel constructs were immunostained with markers selected following recommendations from the Spine Research Interest Group [55]. Following culture, whole constructs were fixed in 4% PFA for 12 min, rinsed with 1X PBS (+Ca, +Mg) twice for 10 min each, and permeabilized with 0.2% TritonX-100 (Sigma-Aldrich). Constructs were blocked with 3.75% bovine serum albumin (MilliporeSigma, Burlington, MA) and 5% goat serum (Thermo Fisher Scientific), and immunolabeled with mouse-anti-N-Cadherin (1:150, Sigma-Aldrich), rabbit-anti-BASP1 (1:150, Abcam, Cambridge, United Kingdom), goat-anti-noggin (1:150, Santa Cruz Biotechnology, Dallas, TX), or Alexa-conjugated phalloidin (1:250, Invitrogen). Concentration-matched isotype controls were used for each antibody. Species-matched AlexaFluor™ (Invitrogen) secondary antibodies were applied using a dilution of 1:250, and cells were counterstained with DAPI (2 μg/mL, Sigma-Aldrich). Mean fluorescence intensity was measured for individual ROIs across conditions and normalized to MFI values of the isotype controls to account for non-specific background signal.

2.5. Gene expression

Gene expression was assayed using qPCR on an Applied Biosystems™ StepOnePlus™ Real-Time PCR System (Software v2.3, Foster City, CA) for a subset of targets associated with the NP cell phenotype [55]. Briefly, 3D cell laden-scaffolds containing 2.5×10^6 cells/mL primary adult human NP cells were homogenized using RLT buffer (Qiagen, Hilden, Germany) +1% mercaptoethanol in a BioSpec Mini-Beadbeater-24 bead beater (BioSpec, Bartlesville, OK) at 3000 rpm using 2 mm diameter zirconia beads (BioSpec), and stored at −80 °C until ready for RNA isolation. RNA was isolated using the QIAGEN™ Mini kit following manufacturer instructions (Qiagen). RNA concentration and purity were determined using the 260/280 ratio quantified via a NanoDrop™ system (ThermoFisher Scientific). RNA was converted to cDNA using the iScript cDNA Synthesis Kit (BioRad, Hercules, CA). RT-qPCR was used to detect amplification of aggrecan (ACAN), collagen 2 (COL2A1), N–Cadherin (CDH2), glucose transporter 1 (GLUT1), connective tissue growth factor (CTGF), brain associated soluble protein 1 (BASP1), integrin $\alpha 6$ (ITGa6), and collagen I (COL1A1) (Supplementary Table 1, Applied Biosystems) by reporting $2^{-\Delta\Delta Ct}$, with the first Δ being normalization of the transcripts for each target gene to housekeeping genes 18S and GAPDH, and the second Δ being the difference between normalized expression for PEG-peptide hydrogel culture and soft PEG-LM positive control [8,33,34].

2.6. In vivo *disc puncture model*

All animal work was done with approval by the Washington University Institutional Animal Care and Use Committee. Male Sprague-Dawley rats ($n = 12$, 10–12 weeks old, Charles River Laboratories, Wilmington, MA) were co-housed (two rats per cage) and allowed to acclimate for one week. On the day of surgery, rats were anesthetized under 1.5–3% isoflurane + 1–2% O_2, and a subcutaneous injection of carprofen (5 mg/kg) [44] was administered prior to the start of the procedure. Caudal discs (C5-C8) were exposed with a ~4 cm incision on the ventral plane of the tail using a size 21 blade to expose the disc levels from C5 to C8. The C5-C6 and C7-C8 discs of all rats were punctured to a depth of 3 mm using a 27 G needle; discs at the C6-C7 level were left without a puncture to serve as the sham control [45]. The incision was then closed using 4–0 nylon sutures. Animals were allowed to recover and returned to co-housing and free ambulatory activity. Food and water were available *ad libitum*, and the rats were kept under a 12/12 light/dark cycle and with a constant room temperature of 21 °C ± 1. Chewable carprofen tablets (dosage of 5 mg/kg) were administered daily for 4 days following surgery. The rats were then monitored for two-weeks post-surgery while allowing for the progression of acute disc degeneration [45,56].

2.7. Cell-laden hydrogel and cell suspension delivery

Following the two-week recovery period, rats were anesthetized using 1.5–3% isoflurane + 1–2% O_2 to expose the caudal IVDs as previously described. Discs C5-C6 received either cell-laden hydrogel or cells-only. For the cell laden hydrogel, one Hamilton syringe (Hamilton Company, Reno, NV) contained 5 μL of the peptide-functionalized PEG-8MAL solution, and a second syringe contained 5 μL of the PEG-dithiol crosslinker prepared with

luciferase-expressing rat NP cells at 5 × 10^6 cells/mL. Both volumes were delivered through a 25 G needle inserted in the left and right aspects of the target IVD (Fig. 5). The needles were left in the disc for 10 s to allow for gel formation and minimize gel extrusion from the disc space. Following mixing and *in situ* crosslinking, the final cell density delivered was thus 2.5 × 10^6 cells/mL, on the lower range of the estimated cell density in the native IVD (~5 × 10^6 cells/mL [4]). A 25 G needle was used for polymer delivery to overcome viscosity issues at smaller gauges. The cell-only condition was likewise administered, with one injection containing the cell suspension and the second injection containing media alone. Discs at the C6-C7 level remained unpunctured to serve as sham controls; discs C7-C8 were punctured an additional two times using a 25 G needle in order to mimic hydrogel delivery conditions without delivering cells or gel. Tail incisions were then closed with 4–0 sutures, and the rats were allowed to recover, receiving chewable carprofen tablets (dosage of 5 mg/kg) daily for 4 days. Rats were sacrificed at two different time points, with the first cohort sacrificed one week following hydrogel delivery (t = 1 week), and the second cohort sacrificed eight weeks following hydrogel delivery (t = 8 weeks).

In order to track cell viability and retention of the delivered cells *in vivo*, rat NP cells were first isolated from multiple caudal discs of Sprague-Dawley rats as described above. Cells were pooled from multiple rats (n = 8) passaged once and expanded to ensure adequate cell numbers. Following, cells were plated at a density of 500,000 cells/well in wells of a 6 well plate in 2 mL transduction media containing 10% FBS, 4 μg/mL polybrene (hexadimethrine bromide, Sigma Aldrich), and 4 μL of the concentrated lentiviral plasmid (titer 5.5 × 10^8) containing a luciferase reporter upstream of the constitutive EF1 promoter (Plasmid #21,375, Addgene, Watertown, MA). Cells were cultured in the transduction media for 20 h, rinsed twice with 1X PBS, and then culture media (F12 + 10% FBS + 1% P/S) was added to the wells. Cells were allowed to recover for at least 24 h. Transduction efficiency was tested by staining with a rabbit-anti-firefly luciferase antibody (Abcam) and quantifying positively labeled cells via flow cytometry (Guava easyCyte flow cytometer, Millipore Sigma). Cells were measured to be efficiently transduced with the LV-EF1-luc containing vector (81% positive cells).

2.8. Tissue harvesting, μCT, and histology

At one- and eight-weeks post hydrogel delivery, rats were sacrificed and the caudal spines were immediately excised. The muscle and tail tendons surrounding the spine were removed, the spines were rinsed in 1X PBS, and then placed in 4% PFA for 48 h with gentle rocking at 4 °C (replaced once after 24 h). Following, the tails were analyzed under μCT using a Bruker SkyScan 1176 (Bruker Corporation, Billerica, MA) at 60 kV, 417 μA, and 65 ms exposure. Disc Height Index (DHI) was calculated by $DHI = \frac{2(A_1+A_2+A_3)}{(B_1+B_2+B_3+B_4+B_5+B_6)}$, where a_x are the measurements of disc height across 3 different points, and B_x are the measurements of the bounding vertebral bodies at three points [57]. Endplate degeneration grading was done as suggested by Ishiguro and co-workers on a scale of 0–3, where 3 corresponds to no evidence of endplate pathology, and 0 corresponds to severe pathology as observed by substantial presence of endplate irregularities and focal defects [7,29]. Following μCT imaging, discs were processed for histological sectioning. Whole spines were first decalcified in 14% (w/v) EDTA pH 7.2 for 7 days at 4 °C with gentle rocking, then cut into individual motion segments and decalcified for an additional 7 days in fresh 14% EDTA [58]. Following, motion segments were cryoprotected in 30% sucrose (24 h, 4 °C), embedded in OCT, snap-frozen in liquid nitrogen and stored at −80 °C until sectioning. Histological sections were taken in the coronal plane at a thickness of 20 μm to preserve hydrogel integrity and prevent gel tearing. In order to measure effective cell localization as well as cell retention within the IVD space following cell-laden hydrogel delivery, sections were stained with a rabbit-anti-luciferase in order to visualize and identify the LV-luc transduced cells delivered to the discs. For qualitative analysis of histological sections, discs were stained with 0.1% safranin-O, 0.02% fast green, and haematoxylin, then overlaid with Permount and coverslipped for imaging. For qualitative study of the phenotypic state of the delivered NP cells, sections were stained with a mouse-anti-N-Cadherin (Abcam), rabbit-anti-BASP1 (Abcam), or rabbit-anti-integrin α6 (Abcam). Sections were counterstained with DAPI for visualization of cell nuclei.

3. Statistical analysis

Statistical analyses were conducted using one-way ANOVA to test for evidence of differences amongst groups unless otherwise noted. All data are expressed as mean ± standard deviation. Analyses were conducted prior to log transformation in qPCR datasets to better satisfy the normality assumption. Gene expression levels were compared between groups by performing t-tests on delta-Ct values as described above. For comparison of treatment groups *in vivo*, one-way ANOVA with Holm-Sidak's multiple comparisons tests were employed, and conducted independently for each timepoint. All statistical analyses were 2-sided, and conducted at significance levels of $p < 0.05$.

4. Results

4.1. Stiff low-peptide functionalized density hydrogels promote cell viability and biosynthetic activity in human NP cells following 3D culture in vitro

Significantly higher cell viability was observed in the stiff low-peptide density (15% 100 μM), stiff-high peptide (15% 400 μM), and soft PEG-laminin (4% PEG-LM) gels than the nonfunctionalized stiff hydrogel control, although there was no evidence of differences amongst the functionalized systems (Fig. 1A). All functionalized systems exhibited significantly higher biosynthetic activity than the stiff non-functionalized control, with the soft PEG-LM gel exhibiting significantly higher rates of biosynthesis than all other conditions (Fig. 1B,D). Soft PEG-LM as well as stiff low-peptide constructs demonstrated significantly higher amounts of extracellular protein deposition than both the stiff-high peptide system and nonfunctionalized controls (Fig. 1C, Supplementary Fig. 1). Evidence of vacuolation could also be observed in cells cultured within the soft PEG-LM and stiff low-peptide density systems (Supplementary Fig. 2).

4.2. Stiff low-peptide functionalized systems promote increased protein deposition and similar gene expression profiles as soft PEG-LM gels for cells in 3D culture in vitro

The stiff low-peptide density hydrogel demonstrated the highest expression of N–Cadherin and noggin of all substrates studied, along with higher proportions of cells expressing these proteins (Fig. 2A,B,D). No difference in expression or in proportions of cells expressing BASP1 were measured between the stiff low-peptide and soft PEG-LM substrates, although these were significantly higher than both the stiff-high and nonfunctionalized groups (Fig. 2C,D).

The soft PEG-LM gel has previously been demonstrated to promote expression of NP cell phenotypic markers including ACAN, BASP1, CDH2, and GLUT1 in adult human NP cells following 2D

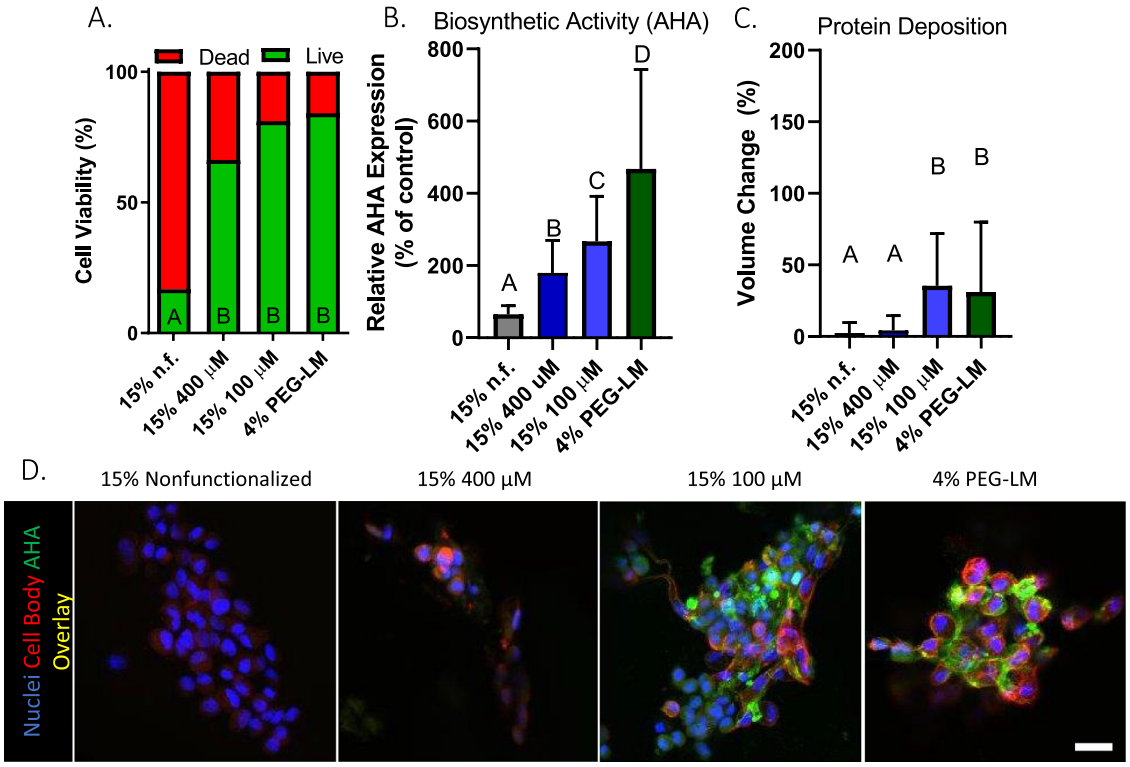

Fig. 1. Functionalized systems support cell viability and biosynthetic activity following 3D culture. (A) Cell viability as quantified by Live/Dead assay. No statistical differences were found in percent viable cells between functionalized substrates, but all were different from nonfunctionalized controls. (B,C) Biosynthetic activity and matrix deposition as measured via functional non-canonical amino acid tagging (FUNCAT) approach shows that both the stiff low peptide and soft PEG-LM substrates promote increased protein production compared to the stiff high peptide and nonfunctionalized controls, with PEG-LM demonstrating the highest biosynthetic activity. (D) Representative images of FUNCAT. For all plots, cells from $n = 5$ independent ROIs for each of $n = 4$ human samples, ages 30–68, both sexes, were measured. Scale bar is 20 μm. Statistical test for all parameters was a one-way ANOVA with Holm-Sidak's multiple comparison's test. Same letter denotes no significance, while different letters denote differences at $p < 0.05$.

and 3D culture [8,33,34]. Therefore, expression profiles of NP cells encapsulated in the stiff low-peptide functionalized gels was compared to cells cultured within soft PEG-LM gels. Gene expression profiles were not surveyed for nonfunctionalized and stiff-high peptide density groups due to their observed low protein expression and increased morphological differences resembling those of a more fibroblast-like phenotype (Supplementary Fig. 3). We observed gene expression of ACAN and CTGF was reduced by the stiff peptide-functionalized gels compared to soft PEG-LM (Fig. 2E). In contrast, CDH2 expression was significantly increased by the stiff low- functionalized gels compared to soft PEG-LM. The data further demonstrated trends towards increased expression of GLUT1 and BASP1 without evidence of statistical significance, and similar expression levels of COL2A1, ITGA6, and COL1A1 between the two hydrogels tested (Fig. 2E).

4.3. Cell laden stiff low-peptide functionalized hydrogel delivery into the rat intradiscal space in vivo *promotes improved DHI and endplate structure*

Based on the *in vitro* findings that the stiff low-peptide functionalized hydrogels supported cell viability and biosynthetic activity at levels similar to or greater than the pro-phenotypic soft PEG-LM, only the stiff low-peptide density system was studied as a cell carrier for delivery into the degenerative IVD. Significantly greater values for disc height index (DHI) were observed in cell-laden hydrogel treated discs compared to the punctured non-treated controls at both the 1-week and 8-week timepoints, and for the cell-only group at the 8-week timepoint (Fig. 3A,B). However, the cell-laden hydrogel delivery group did exhibit significantly lower DHI's compared to the sham (non-punctured) controls. μCT imaging further revealed differences in endplate structure between the conditions (Fig. 3A,C). Semi-quantitative grading of the endplates [29] suggested improved endplate scores in the cell-laden hydrogel treatment group compared to the punctured controls and the cell-only treatment at chronic timepoints. The puncture and cell-only conditions exhibited significant degrees of tissue disruption, anisotropy, and focal defects, which were less pronounced in either the sham or the cell-laden hydrogel groups (Fig. 3A,C).

4.4. Cell-laden hydrogel delivery promotes improved disc phenotype

Increased presence of luciferase+ cells in the cell-laden hydrogel delivery condition confirmed effective delivery and retention of rat NP cells into the intradiscal space (Supplementary Fig. 4). Discs from the puncture and cell-only groups exhibited disorganized endplates with irregularities and focal defects, reduced AF organization, and fibrotic changes to the NP at both time points (Figs. 3A and 4A). Furthermore, histology suggested a decrease in cellularity within the central region of the punctured non-treated discs, and little cell retention in the cell-only controls (Fig. 4, Supplementary Fig. 4). By contrast, endplates in the discs from the cell-laden hydrogel delivery group at both time points exhibited organized structures and more closely resembled the endplates from the sham group than those of the punctured discs. Furthermore, while alterations in AF organization can be observed (likely as a result of the initial puncture insult), distinct lamella remain observable in the cell-laden hydrogel treated group at both timepoints. Lastly, the cell-laden hydrogel delivery group at the 8 week

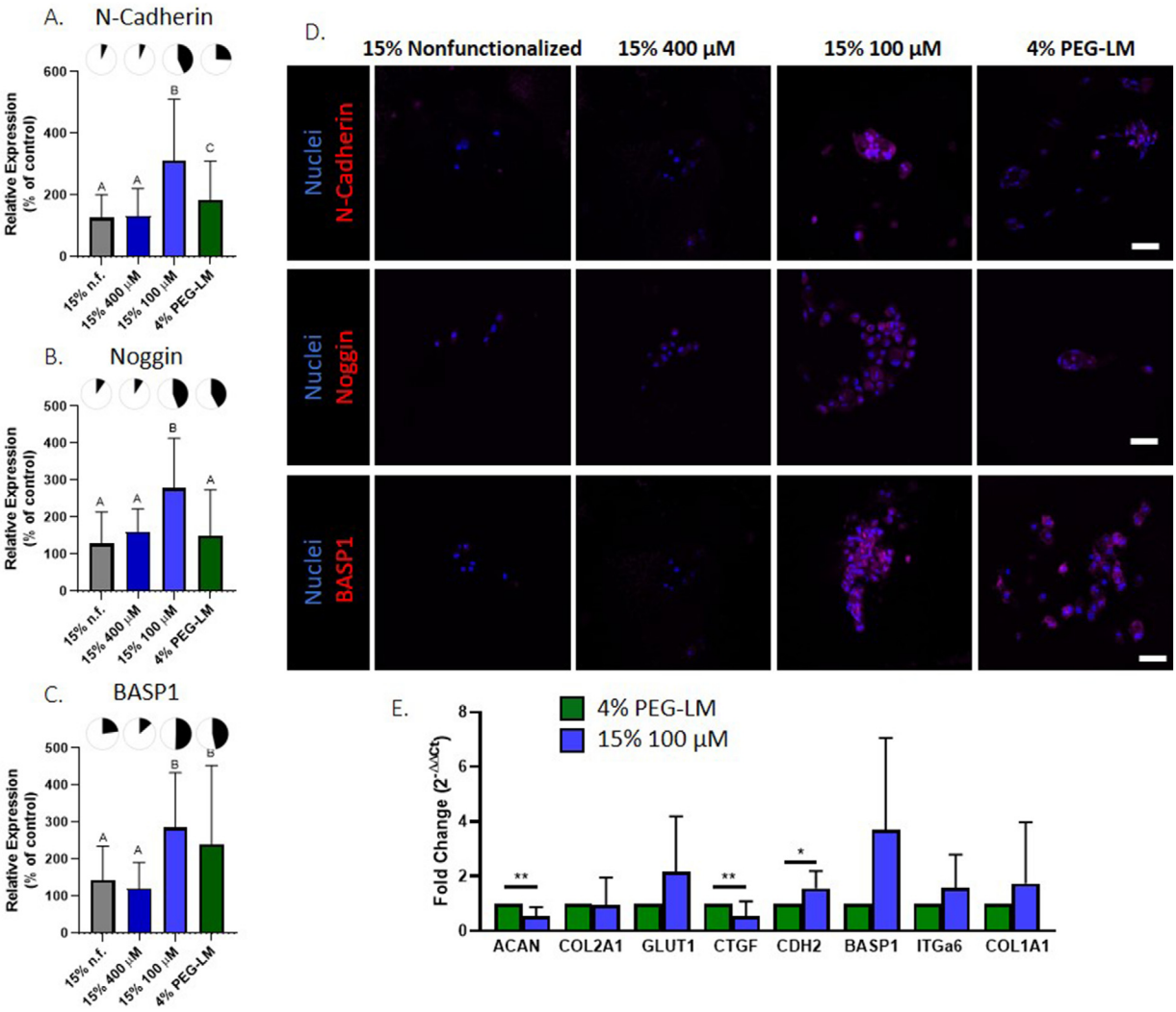

Fig. 2. Stiff low peptide and soft PEG-LM systems promote increases in protein expression. Cells cultured within stiff low peptide density hydrogels expressed significantly higher levels of N–Cadherin (A,D) and noggin (B,D) than any other substrate, and significantly higher amounts of BASP1 (C,D) than both the stiff non-functionalized (control) and stiff-high density substrates though no different than the soft PEG-LM. Stiff low peptide system further suggests higher proportions of cells expressing all of these proteins than either the stiff high peptide and stiff non-functionalized system as shown by the pie-chart insets. (E) Survey of gene expression profiles comparing the stiff-low peptide to the soft PEG-LM control. For A–C, $n > 60$ ROIs from $n = 4$ human samples, ages 30–68, both sexes. Statistical tests for protein expression values were one-way ANOVAs with Holm-Sidak's multiple comparison's test. Same letter denotes no significance between conditions, different letter denotes $p < 0.05$. Scale bar is 50 μm. For (E) statistical tests were t-tests of the $\Delta\Delta C_t$ values comparing the stiff low peptide to the soft PEG-LM for each gene. * is $p < 0.05$, ** is $p < 0.01$.

time point demonstrated increased Safranin-O staining within the central region of the disc, which was not observed in the punctured controls at either time point, nor in the hydrogel delivery group at the one week time point. This may be indicative of cell viability and biosynthetic activity throughout the course of the study, although it may further suggest a longer time required for cells to adapt to their microenvironment following *in vivo* delivery. Histological assessment of the sham discs demonstrated tissue organization and structure consistent with healthy IVDs.

Immunostaining for BASP1, N–Cadherin, and integrin α6 revealed protein presence in both the sham control as well as the hydrogel treated NP regions, while little staining was observed in the punctured NP sections (Fig. 4B). Notably, cellularity appeared strongly reduced in the punctured conditions, potentially playing a role in the apparent decrease in protein expression in these tissues. Although trends suggesting higher protein expression in the cell-laden hydrogel group than in the puncture group were observed at both time points, the relative protein expression in the cell-laden hydrogel conditions appeared qualitatively higher at the 8-week time point than the 1-week time point, particularly with respect to expression levels of integrin α6 and N–Cadherin (Supplementary Fig. 5). These observations may be further suggestive of cells needing a recovery period following intradiscal delivery prior to recovering a biosynthetic phenotype.

5. Discussion

In prior work, full-length laminin-functionalized soft biomaterials were observed to promote shifts in expression of a panel of markers associated with the juvenile NP cell phenotype [8,33,34,59]. While attractive as a bioactive material, this approach poses difficulties due to the size and complexity of the full-length protein [34,60]. Use of laminin-mimetic peptides offers advantages in terms of increased specificity for cell engagement and ligand-receptor interactions, and spatial control over ligand presentation [40,48]. Furthermore, development of stiff biomaterials may be favorable for *in vivo* delivery due to the increased mechanical support to the disc. While materials made from native proteins such as collagen and hyaluronan present cell adhesive ligands that may support NP cell function, these materials suffer from a dependence

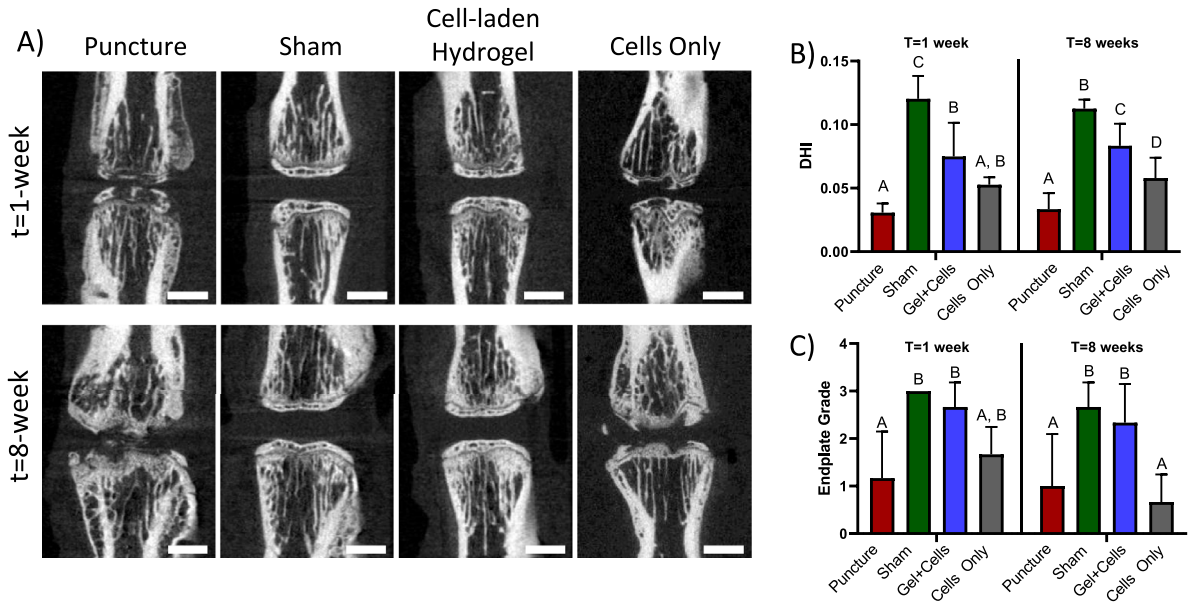

Fig. 3. Radiographic evaluation of the coccygeal spine. (A) µCT scans of the discs show significantly higher disc height index (DHI) in the hydrogel delivery conditions compared to the punctured non treated discs. (B) At both the 1 and 8 week timepoints, DHI in cell-laden hydrogel delivery conditions compared to sham discs is significantly lower, although both DHI and endplate scores (C) in hydrogel delivery conditions are either trending towards or significantly higher than those in the punctured non treated control and cell-only conditions. $n = 6$ rats per condition per timepoint. Scale bars in A are 2 mm. Statistics for B and C were one-way ANOVAs with Holm-Sidak's multiple comparisons test. * $p < 0.05$, ** $p < 0.01$, *** $p < 0.001$, ****$p < 0.0001$.

on full-length proteins as does our earlier work with laminins. Other groups have used peptide-functionalized materials such as the VitroGel 3D RGD modified hydrogel or the synthetic P_{11} peptide:GAG self-assembling hydrogels to facilitate cell delivery and promote tissue repair [61,62]. The tunability of these synthetic systems provides the ability to independently control modalities such as adhesive domain selection, availability, and spatial presentation. The current system further builds upon these findings by engaging integrin- and syndecan-binding domains, the co-presentation of which has previously been demonstrated to promote synergistic adhesive effects and to have significant effects on NP phenotypic modulation [40]. As such, in the present study we examined the potential for a stiff dual peptide-functionalized hydrogel to be used as a cell-carrier for delivery into the degenerative intradiscal space in order to increase disc height and promote cell matrix deposition and tissue integration.

In 3D *in vitro* culture, all functionalized biomaterials tested appeared to promote similar degrees of cell viability, although the stiff biomaterial functionalized with a high peptide density was observed to have significantly lower biosynthetic activity than both the stiff low-peptide and soft PEG-LM systems. Lower degrees of protein expression were further observed in the stiff-high peptide density system than either the stiff low-or soft PEG-LM, which is likely associated with the observed changes in biosynthetic activity. Cells cultured within the stiff low-peptide functionalized gels exhibited the highest protein expression of N–Cadherin (important for regulating cell-cell interactions [63]) and noggin (important in notochordal patterning [64]) among all substrates studied, and exhibited expression levels of BASP1 that were similar to that seen in the soft PEG-LM positive controls. An unexpected observation was the formation of cytosolic vacuoles in 3D culture of adult human NP cells within both the soft PEG-LM and stiff low-peptide density hydrogels, while no vacuolation was observed in either the nonfunctionalized nor the stiff high peptide density groups (Supplementary Fig. 2). This observation is of interest because AHA staining within vacuolar structures appeared modest at best, which may support the hypothesis that vacuoles play a more important role in regulation of intracellular pressure than in molecular transport [65–67]. However, further assessments need to be conducted to better understand these findings and their implications. Together these data validate the stiff biomaterial functionalized with laminin mimetic peptides as a bioactive scaffold capable of promoting cellular behaviors similar to the soft PEG-LM hydrogel during 3D *in vitro* culture. The use of chemically functionalized synthetic polymer systems for cell encapsulation supports the independent control of different material parameters such as hydrogel stiffness and degree of functionalization. This allows for the creation of a stiff biomaterial with reduced peptide density, parameters which are difficult to achieve using naturally occurring materials. In natural polymer systems, adhesive domains (*e.g.* RGD in the case of collagen) are inherently linked to the fiber density [68–70]. Thus, an increase in polymer density results in both a stiffer substrate and an increase in adhesive ligand domain availability. The ability to precisely control both parameters is important, as the controlled presentation of ligands in the stiff polymers has been previously observed to lead to significant changes in phenotypic marker expression [40].

Having validated biomaterials in 3D *in vitro* culture, we then assessed the effects of injecting the cell-laden peptide-functionalized system as a therapeutic to discs degenerated via disc puncture in a rat model of degeneration. *In vivo* delivery of the peptide-functionalized *in situ* crosslinked cell-laden hydrogel promoted significantly higher DHI values compared to the puncture and the cell-only groups, although these values remained significantly lower than in the sham control. µCT analysis further suggested significant changes in endplate organization, with the cell-laden hydrogel group promoting significantly higher degrees of endplate organization than the puncture group, while not being significantly different than the sham group. The peptide-functionalized hydrogel also promoted cell phenotype and exhibited bioactive properties *in vivo* as characterized by increased expression of integrin $\alpha 6$, N–Cadherin, and BASP1, as well as increased Safranin-O pres-

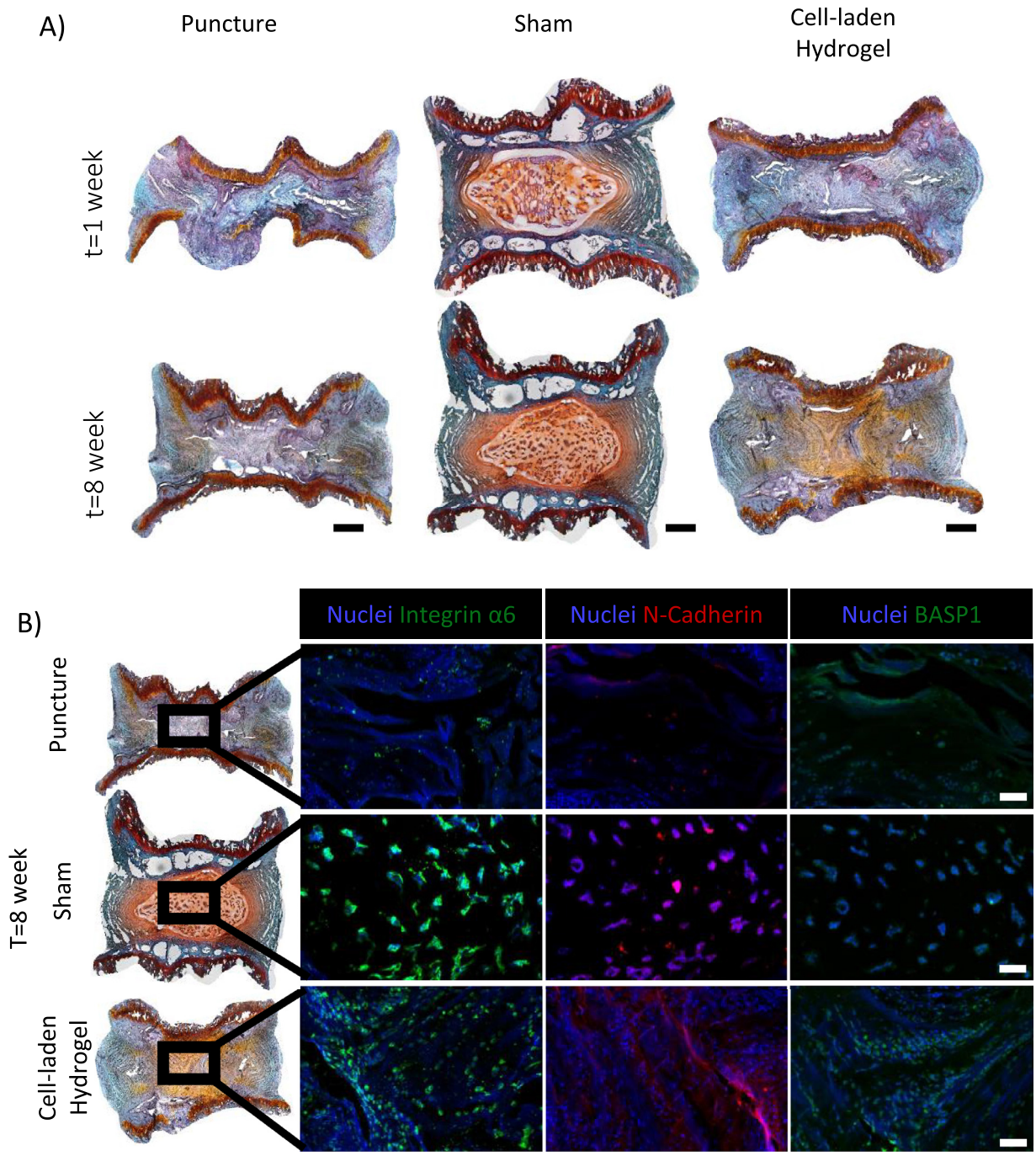

Fig. 4. Histological assessments of the IVDs. (A) 20 μm thick tissue sections, stained via Saf-O/Fast Green/Haematoxylin. Scale bar is 500 μm. (B) At the eighth week post-injury timepoint, differences in protein expression levels between groups was apparent. Although protein expression in the cell-laden hydrogel condition appeared to resemble that of the naïve condition, morphological differences in cell distribution could still be observed. Scale bar is 250 μm. (For interpretation of the references to color in this figure legend, the reader is referred to the web version of this article.)

ence within the central region of the disc, compared to the punctured group. Differences in disc phenotype between the 1-week and 8-week conditions for the cell-laden hydrogel delivery group were observed. Specifically, at $t = 8$ weeks, there was observable Safranin-O staining within the central region of the disc, as well as observable protein expression; however, these characteristics were not observed at the 1-week time point (Supplementary Fig. 5). This may be due to cells requiring a longer time to reach steady state *in vivo* than *in vitro*. Following *in vivo* delivery, cells which were previously cultured in monolayer experience an increase in dimensionality which leads to temporal and spatial alterations to nutrient accessibility, oxygen gradients, and more. The hypoxic and low nutrient disc environment *in vivo* further presents stresses to the delivered cells, which may further result in a slow rate of recovery that leads to longer times being necessary for cells to express the phenotypes observed *in vitro* [71,72].

As suggested in the schematic from Fig. 5, we hypothesize that the *in situ* crosslinked system may act in a defect filling manner with the crosslinked hydrogel becoming entrapped in voids in the nucleotomized disc and the collapsed anular fibers. Both the treated and non-treated discs which underwent puncture show anular disruption and disorganization at early timepoints. This sug-

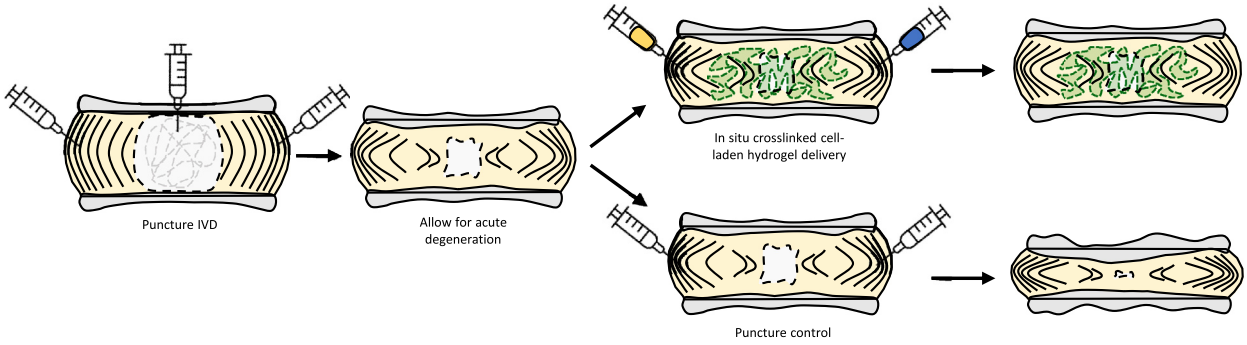

Fig. 5. Hydrogel delivery schematic. Representative schematic of the hypothesized workflow outlining the degrees of degeneration following disc punctures and the *in situ* crosslinked cell-laden hydrogel implant.

gests that although the mechanical support provided by the hydrogel may be sufficient to increase disc height and vertebral body separation, it may not provide sufficient intradiscal pressure to entirely mimic the healthy NP and counteract the AF buckling which results from the puncture injury [73,74]. This is further supported by the observation that, particularly at the 8-week timepoint, the endplates in the treated condition appear healthy and similar to the sham control while the endplates in the non-treated punctured discs show signs of severe degeneration. This finding may suggest that the stiff hydrogel provides help to attenuate endplate damage resulting from disc collapse [11,75]. However, two important shortcomings of this work include the lack of mechanical characterization of the material, and the different needle gauges used for induction of degeneration and therapeutic delivery. In terms of needle dimensions, controls could be better implemented in order to assess any differential effects that may arise from the puncture used for cell-laden hydrogel delivery when compared to the initial disc puncture. Specifically, a control using a single disc puncture would better allow for characterization of background degeneration, and may thus provide better insight as to the effects of hydrogel delivery, thereby strengthening the reported findings. For material characterization, studies such as fatigue performance in cyclical repetitive loading, or of material migration or extrusion in compression and bending tests, would all be required to better assess the integration of the mechanical properties of the hydrogel with the native tissue in order to determine its feasibility as a cell carrier and to further elucidate the role of the hydrogel implant in modifying mobility of the motion segments.

Together, the data from the present study suggest an ability to use the stiff low-peptide density functionalized PEG hydrogel scaffold for efficient 3D encapsulation and cell delivery into the degenerative disc space. Results from both *in vivo* and *in vitro* culture validate the system as an effective cell carrier capable of promoting cell retention within the IVD, and able to provide cells with cues critical for promoting cell viability, increased biosynthetic activity, matrix deposition, and protein expression. The benefit of the cell-laden construct appeared to be most prominent at the 8-week timepoint, suggesting that the biomaterial construct may promote sustained structural and phenotypic shifts following the initiation of tissue degeneration. Nevertheless, the findings are confined to our use of primary cells, while alternate cell sources may be better suited to clinical translation.

Declaration of Competing Interest

The authors declare that they have no known competing financial interests or personal relationships that could have appeared to influence the work reported in this paper.

CRediT authorship contribution statement

Marcos N. Barcellona: Conceptualization, Formal analysis, Data curation, Writing – original draft, Writing – review & editing. **Julie E. Speer:** Conceptualization, Formal analysis, Data curation, Writing – review & editing. **Liufang Jing:** Writing – review & editing. **Deepanjali S. Patil:** Writing – review & editing. **Munish C. Gupta:** Data curation, Writing – review & editing. **Jacob M. Buchowski:** Data curation, Writing – review & editing. **Lori A. Setton:** Conceptualization, Formal analysis, Data curation, Writing – review & editing.

Acknowledgements

This material is based upon work supported by grants from the National Science Foundation (Grant No. DGE-1745038), National Institutes of Health (AR069588, AR077678, AR070975), and the Olin Fellowship Foundation at Washington University in St. Louis. Any opinions, findings, and conclusions or recommendations expressed in this material are those of the author(s).

Supplementary materials

Supplementary material associated with this article can be found, in the online version, at doi:10.1016/j.actbio.2021.06.045.

References

[1] J.C. Iatridis, L.A. Setton, M. Weidenbaum, V.C. Mow, Alterations in the mechanical behavior of the human lumbar nucleus pulposus with degeneration and aging, J. Orthop. Res. 15 (1997) 318–322.
[2] P.J. Roughley, Biology of intervertebral disc aging and degeneration: involvement of the extracellular matrix, Spine (Phila. Pa. 1976) 29 (2004) 2691–2699.
[3] M.A. Adams, P.J. Roughley, What is intervertebral disc degeneration, and what causes it?, in: Spine (Phila. Pa. 1976), 31, 2006, pp. 2151–2161.
[4] J.P.G. Urban, S. Roberts, Degeneration of the intervertebral disc, Arthritis Res. Ther. 5 (2003) 120–130.
[5] W.C.W. Chan, K.L. Sze, D. Samartzis, V.Y.L. Leung, D. Chan, Structure and biology of the intervertebral disk in health and disease, Orthop. Clin. North Am. 42 (2011) 447–464.
[6] L.A. Setton, Mechanobiology of the intervertebral disc and relevance to disc degeneration, J. Bone Jt. Surg. 88 (2006) 52.
[7] N. Boos, S. Weissbach, H. Rohrbach, C. Weiler, K.F. Spratt, A.G. Nerlich, Classification of age-related changes in lumbar intervertebral discs, Spine (Phila. Pa. 1976) 27 (2002) 2631–2644.
[8] B.V. Fearing, L. Jing, M.N. Barcellona, S.E. Witte, J.M. Buchowski, L.P. Zebala, M.P. Kelly, S. Luhmann, M.C. Gupta, A. Pathak, L.A. Setton, Mechanosensitive transcriptional coactivators MRTF-A and YAP/TAZ regulate nucleus pulposus cell phenotype through cell shape, FASEB J. 33 (2019) 14022–14035.
[9] J.C. Iatridis, M. Weidenbaum, L.A. Setton, V.C. Mow, Is the nucleus pulposus a solid or a fluid? Mechanical behaviors of the nucleus pulposus of the human intervertebral disc, Spine (Phila. Pa. 1976) 21 (1996) 1174–1184.
[10] J.M. Cloyd, N.R. Malhotra, L. Weng, W. Chen, R.L. Mauck, D.M. Elliott, Material properties in unconfined compression of human nucleus pulposus, injectable hyaluronic acid-based hydrogels and tissue engineering scaffolds, Eur. Spine J. 16 (2007) 1892–1898.

[11] B.A. Walter, P. Mageswaran, X. Mo, D.J. Boulter, H. Mashaly, X.V. Nguyen, L.M. Prevedello, W. Thoman, B.D. Raterman, P. Kalra, E. Mendel, W.S.. Marras, A. Kolipaka, MR elastography-derived stiffness: a biomarker for intervertebral disc degeneration, Radiology 285 (2017) 167–175.
[12] G. Pattappa, Z. Li, M. Peroglio, N. Wismer, M. Alini, S. Grad, Diversity of intervertebral disc cells: phenotype and function, J. Anat. 221 (2012) 480–496.
[13] A.J. Freemont, T.E. Peacock, P. Goupille, J.A. Hoyland, J. O'Brien, M.I.V Jayson, Nerve ingrowth into diseased intervertebral disc in chronic back pain, Lancet 350 (1997) 178–181.
[14] J. Chen, L. Jing, C.L. Gilchrist, W.J. Richardson, R.D. Fitch, L.A. Setton, Expression of laminin isoforms, receptors, and binding proteins unique to nucleus pulposus cells of immature intervertebral disc, Connect. Tissue Res. 50 (2009) 294–306.
[15] J.J. Trout, J.A. Buckwalter, K.C. Moore, S.K. Landas, Ultrastructure of the human intervertebral disc. I. changes in notochordal cells with age, Tissue Cell 14 (1982) 359–369.
[16] C. Woiciechowsky, A. Abbushi, M.L. Zenclussen, P. Casalis, J.P. Krüger, U. Freymann, M. Endres, C. Kaps, Regeneration of nucleus pulposus tissue in an ovine intervertebral disc degeneration model by cell-free resorbable polymer scaffolds, J. Tissue Eng. Regen. Med. 10 (2014) 811–820, doi:10.1002/term.
[17] R.D. Bowles, R.M. Williams, W.R. Zipfel, L.J. Bonassar, Self-assembly of aligned tissue-engineered annulus and intervertebral disc composite via collagen gel contraction, Tissue Eng. Part A 16 (2010) 1339–1348.
[18] H. Mizuno, A.K. Roy, C.A. Vacanti, K. Kojima, M. Ueda, L.J. Bonassar, Tissue-engineered composites of anulus fibrosus and nucleus pulposus for intervertebral disc replacement, *Spine (Phila. Pa.* 1976) 29 (2004) 1290–1297.
[19] S.J. Bidarra, C.C. Barrias, P.L. Granja, Injectable alginate hydrogels for cell delivery in tissue engineering, Acta Biomater 10 (2014) 1646–1662.
[20] D. Rajesh, C.L. Dahia, Role of sonic hedgehog signaling pathway in intervertebral disc formation and maintenance, Curr. Mol. Biol. Rep. 4 (2019) 173–179.
[21] A.G. Nerlich, R. Schaaf, B. Walchli, N. Boos, Temporo-spatial distribution of blood vessels in human lumbar intervertebral discs, Eur. Spine J. 16 (2006) 547–555.
[22] L.I. Kauppila, Ingrowth of blood vessels in disc degeneration, J. Bone Jt. Surg. 77 (1995) 26–31.
[23] A. Maroudas, R.A. Stockwell, A. Nachemson, J. Urban, Factors involved in the nutrition of the human lumbar intervertebral disc: cellularity and diffusion of glucose *in vitro*, J. Anat. 120 (1975) 113–130.
[24] T. Tsujimoto, H. Sudo, M. Todoh, K. Yamada, K. Iwasaki, T. Ohnishi, N. Hirohama, T. Nonoyama, D. Ukeba, K. Ura, Y.M. Ito, N. Iwasaki, EBioMedicine An acellular bioresorbable ultra-puri fi ed alginate gel promotes intervertebral disc repair : a preclinical proof-of-concept study, EBioMedicine 37 (2018) 521–534.
[25] A.A. Thorpe, G. Dougill, L. Vickers, N.D. Reeves, C. Sammon, G. Cooper, C.L.Le Maitre, Thermally triggered hydrogel injection into bovine intervertebral disc tissue explants induces differentiation of mesenchymal stem cells and restores mechanical function, Acta Biomater 54 (2017) 212–226.
[26] S.E. Gullbrand, T.P. Schaer, P. Agarwal, J.R. Bendigo, G.R. Dodge, W. Chen, D.M. Elliott, R.L. Mauck, R. Neil, L.J. Smith, Translation of an injectable triple-interpenetrating-network hydrogel for intervertebral disc regeneration in a goat model, Acta Biomater. (2017) 201–209, doi:10.1016/j.actbio.2017.07.025.T.
[27] G. Vadala, G. Sowa, M. Hubert, L.G. Gilbertson, V. Denaro, J.D. Kang, Mesenchymal stem cells injection in degenerated intervertebral disc : cell leakage may induce osteophyte formation, J. Tissue Eng. Regen. Med. 6 (2012) 348–355.
[28] V. Tam, I. Rogers, D. Chan, V.Y.L. Leung, K.M.C Cheung, A Comparison of intravenous and intradiscal delivery of multipotential stem cells on the healing of injured intervertebral disk architecture nor the disk height index, J. Orthop. Res. (2014) 819–825, doi:10.1002/jor.22605.
[29] H. Ishiguro, T. Kaito, S. Yarimitsu, K. Hashimoto, R. Okada, J. Kushioka, R. Chijimatsu, S. Takenaka, T. Makino, Y. Sakai, Y. Moriguchi, S. Otsuru, D.A. Hart, H. Fujie, N. Nakamura, H. Yoshikawa, Intervertebral disc regeneration with an adipose mesenchymal stem cell-derived tissue-engineered construct in a rat nucleotomy model, Acta Biomater. 87 (2019) 118–129.
[30] G. Crevensten, A.J.L. Walsh, D. Ananthakrishnan, P. Page, G.M. Wahba, J.C. Lotz, S. Berven, Intervertebral disc cell therapy for regeneration: mesenchymal stem cell implantation in rat intervertebral discs, Ann. Biomed. Eng. 32 (2004) 430–434.
[31] L.J. Smith, L. Silverman, D. Sakai, C.L. Le Maitre, R.L. Mauck, N.R. Malhotra, J.C. Lotz, C.T. Buckley, Advancing cell therapies for intervertebral disc regeneration from the lab to the clinic: recommendations of the ORS spine section, JOR Spine 1 (2018).
[32] H. Bertram, M. Kroeber, H. Wang, F. Unglaub, T. Guehring, C. Carstens, W. Richter, Matrix-assisted cell transfer for intervertebral disc cell therapy, Biochem. Biophys. Res. Commun. 331 (2005) 1185–1192.
[33] A.T. Francisco, R.J. Mancino, R.D. Bowles, J.M. Brunger, D.M. Tainter, Y.Te Chen, W.J. Richardson, F. Guilak, L.A Setton, Injectable laminin-functionalized hydrogel for nucleus pulposus regeneration, Biomaterials 34 (2013) 7381–7388.
[34] A.T. Francisco, P.Y. Hwang, C.G. Jeong, L. Jing, J. Chen, L.A. Setton, Photocrosslinkable laminin-functionalized polyethylene glycol hydrogel for intervertebral disc regeneration, Acta Biomater. 10 (2014) 1102–1111.
[35] A.A. Thorpe, C. Sammon & C.L. Le Maitre ' Cell or not to cell ' that is the question: for intervertebral disc regeneration? J. Stem Cells Res. Dev. Ther. 2 (2015).
[36] S.E. Gullbrand, B.G. Ashinsky, E.D. Bonnevie, D.H. Kim, J.B. Engiles, L.J. Smith, D.M. Elliott, T.P. Schaer, H.E. Smith, R.L. Mauck, Long-term mechanical function and integration of an implanted tissue-engineered intervertebral disc, Sci. Transl. Med. 10 (2018) 1–11.
[37] D. Sakai, J. Mochida, Y. Yamamoto, T. Nomura, M. Okuma, K. Nishimura, T. Nakai, K. Ando, T. Hotta, Transplantation of mesenchymal stem cells embedded in atelocollagen gel to the intervertebral disc: a potential therapeutic model for disc degeneration, Biomaterials 24 (2003) 3531–3541.
[38] L.J. Smith, D.J. Gorth, B.L. Showalter, J.A. Chiaro, E.E. Beattie, D.M. Elliott, R.L. Mauck, W. Chen, N.R. Malhotra, *In vitro* characterization of a stem-cell-seeded triple-interpenetrating- network hydrogel for functional regeneration of the nucleus pulposus, Tissue Eng. Part A 20 (2014) 1841–1849.
[39] T.C. Schmitz, E. Salzer, J.F. Crispim, G.T. Fabra, C. LeVisage, A. Pandit, M. Tryfonidou, C. Le Maitre, K. Ito, Characterization of biomaterials intended for use in the nucleus pulposus of degenerated intervertebral discs, Acta Biomater. 114 (2020) 1–15.
[40] M.N. Barcellona, J.E. Speer, B.V. Fearing, L. Jing, A. Pathak, M.C. Gupta, J.M. Buchowski, M. Kelly, L.A Setton, Control of adhesive ligand density for modulation of nucleus pulposus cell phenotype, Biomaterials 250 (2020) 120057.
[41] D.T. Bridgen, C.L. Gilchrist, W.J. Richardson, R.E. Isaacs, C.R. Brown, K.L. Yang, J. Chen, L.A. Setton, Integrin-mediated interactions with extracellular matrix proteins for nucleus pulposus cells of the human intervertebral disc, J. Orthop. Res. 31 (2014) 1–14.
[42] J.T. Martin, D.J. Gorth, E.E. Beattie, B.D. Harfe, L.J. Smith, D.M. Elliott, Needle puncture injury causes acute and long-term mechanical deficiency in a mouse model of intervertebral disc degeneration, J. Orthop. Res. 31 (2013) 1276–1282.
[43] C.L. Korecki, J.J. Costi, J.C. Iatridis, Needle puncture injury affects intervertebral disc mechanics and biology in an organ culture model, Spine (Phila. Pa. 1976) 33 (2008) 235–241.
[44] I.L. Mohd Isa, S.A. Abbah, M. Kilcoyne, D. Sakai, P. Dockery, D.P. Finn, A. Pandit, Implantation of hyaluronic acid hydrogel prevents the pain phenotype in a rat model of intervertebral disc injury, Sci. Adv. (2018) 1–20.
[45] E.M. Leimer, M.G. Gayoso, L. Jing, S.Y. Tang, M.C. Gupta, L.A. Setton, Behavioral compensations and neuronal remodeling in a rodent model of chronic intervertebral disc degeneration, Sci. Rep. 9 (2019) 1–10.
[46] K. Masuda, Y. Aota, C. Muehleman, Y. Imai, M. Okuma, E.J. Thonar, G.B. Andersson, H.S. An, A novel rabbit model of mild, reproducible disc degeneration by an anulus needle puncture: correlation between the degree of disc injury and radiological and histological appearances of disc degeneration, Spine (Phila. Pa. 1976) 30 (2005) 5–14.
[47] E. Nilsson, T. Nakamae, K. Olmarker, Pain behavior changes following disc puncture relate to nucleus pulposus rather than to the disc injury per se : an experimental study in rats, Open Orthop. J. 5 (2011) 72–77.
[48] D.T. Bridgen, B.V. Fearing, L. Jing, J. Sanchez-Adams, M.C. Cohan, F. Guilak, J. Chen, L.A. Setton, Regulation of human nucleus pulposus cells by peptide–coupled substrates, Acta Biomater. 55 (2017) 100–108.
[49] H.E. Gruber, E.N. Hanley, Human disc cells in monolayer *vs* 3D culture: cell shape, division and matrix formation, BMC Musculoskelet. Disord. 1 (2000) 1–6.
[50] E.A. Phelps, N.O. Enemchukwu, V.F. Fiore, J.C. Sy, N. Murthy, T.A. Sulchek, T.H. Barker, A.J. García, Maleimide cross-linked bioactive PEG hydrogel exhibits improved reaction kinetics and cross-linking for cell encapsulation and *in situ* delivery, Adv. Mater. 24 (2012) 64–70.
[51] N.O. Enemchukwu, R. Cruz-Acuña, T. Bongiorno, C.T. Johnson, J.R. García, T. Sulchek, A.J. García, Synthetic matrices reveal contributions of ECM biophysical and biochemical properties to epithelial morphogenesis, J. Cell Biol. 212 (2016) 113–124.
[52] B.V. Fearing, P.A. Hernandez, L.A. Setton, N.O. Chahine, Mechanotransduction and cell biomechanics of the intervertebral disc, JOR Spine 1 (2018) e1026.
[53] C.M. Mcleod, R.L. Mauck, High fidelity visualization of cell- to-cell variation and temporal dynamics in nascent extracellular matrix formation, Nat. Sci. Rep. 6 (2016).
[54] C. Dunham, N. Havlioglu, A. Chamberlain, S. Lake, G. Meyer, Adipose stem cells exhibit mechanical memory and reduce fibrotic contracture in a rat elbow injury model, FASEB J. 34 (2020) 12976–12990.
[55] M.V. Risbud, Z.R. Schoepflin, F. Mwale, R.A. Kandel, S. Grad, J.C. Iatridis, D. Sakai, J.A. Hoyland, Defining the phenotype of young healthy nucleus pulposus cells: recommendations of the spine research interest group at the 2014 annual ors meeting, J. Orthop. Res. 33 (2015) 283–293.
[56] M. Miyagi, T. Ishikawa, S. Orita, Y. Eguchi, H. Kamoda, G. Arai, M. Suzuki, G. Inoue, Y. Aoki, T. Toyone, K. Takahashi, S. Ohtori, Disk injury in rats produces persistent increases in pain-related neuropeptides in dorsal root ganglia and spinal cord glia but only transient increases in inflammatory mediators: pathomechanism of chronic diskogenic low back pain, in: Spine (Phila. Pa. 1976), 36, 2011, pp. 2260–2266.
[57] K. Vincent, S. Mohanty, R. Pinelli, P. Pricop, T.J. Albert, C.L. Dahia, Aging of mouse intervertebral disc and association with back pain, Bone 123 (2019) 246–259.
[58] A. Binch, J. Snuggs, C.L. Le Maitre, Immunohistochemical analysis of protein expression in formalin fixed paraffin embedded human intervertebral disc tissues, JOR Spine 3 (2020) 1–9.
[59] C.L. Gilchrist, E.M. Darling, J. Chen, L.A. Setton, Extracellular matrix ligand and stiffness modulate immature nucleus pulposus cell-cell interactions, PLoS ONE 6 (2011).
[60] Y. Kikkawa, K. Hozumi, F. Katagiri, M. Nomizu, H.K. Kleinman, J.E. Koblinski, Laminin-111-derived peptides and cancer, Cell Adhes. Migr. 7 (2013) 150–159.
[61] F. Wang, L. Nan, S. Zhou, Y. Liu, Z. Wang, J. Wang, X. Feng, L. Zhang, Injectable hydrogel combined with nucleus pulposus-derived mesenchymal stem cells for the treatment of degenerative intervertebral disc in rats, Stem Cells Int. (2019).

[62] D.E. Miles, E.A. Mitchell, N. Kapur, P.A. Beales, R.K. Wilcox, Peptide:glycosaminoglycan hybrid hydrogels as an injectable intervention for spinal disc degeneration, J. Mater. Chem. B. Mater. Biol. Med. 4 (2016) 3225–3231.
[63] P.Y. Hwang, L. Jing, K.W. Michael, W.J. Richardson, J. Chen, L.A. Setton, N-Cadherin-mediated signaling regulates cell phenotype for nucleus pulposus cells of the intervertebral disc, Cell Mol. Bioeng. 8 (2015) 51–62.
[64] D. Purmessur, C.C. Guterl, S.K. Cho, M.C. Cornejo, Y.W. Lam, B.A. Ballif, D.M. Laudier, J.C. Iatridis, Dynamic pressurization induces transition of notochordal cells to a mature phenotype while retaining production of important patterning ligands from development, Arthritis Res. Ther. 15 (2013) R122.
[65] X. Hong, C. Zhang, F. Wang, X.-.T. Wu, Large cytoplasmic vacuoles within notochordal nucleus pulposus cells : a possible regulator of intracellular pressure that shapes the cytoskeleton and controls proliferation, Cells Tissues Organs 206 (2018) 9–15.
[66] L. Resutek, A.H. Hsieh, The vacuolated morphology of chordoma cells is dependent on cytokeratin intermediate filaments, J. Cell. Physiol. 234 (2018) 3458–3468, doi:10.1002/jcp.26809.
[67] F. Wang, Z.X. Gao, F. Cai, A. Sinkemani, Z.Y. Xie, R. Shi, J.N. Wei, X.T. Wu, Formation, function, and exhaustion of notochordal cytoplasmic vacuoles within intervertebral disc : current understanding and speculation, Oncotarget 8 (2017) 57800–57812.
[68] N.O. Enemchukwu, R. Cruz-Acuña, T. Bongiorno, C.T. Johnson, J.R. García, T. Sulchek, A.J. García, Synthetic matrices reveal contributions of ECM biophysical and biochemical properties to epithelial morphogenesis, J. Cell Biol. 212 (2016) 113–124.
[69] L.E. O'Brien, M.M.P. Zegers, K.E. Mostov, Building epithelial architecture: insights from three-dimensional culture models, Nat. Rev. Mol. Cell Biol. 3 (2002).
[70] R. Mroue, M.J. Bissell, Three-dimensional cultures of mouse mammary epithelial cells, Methods Mol. Biol. 945 (2013) 221–250.
[71] A. Hiyama, R. Skubutyte, D. Markova, D.G. Anderson, S. Yadla, D. Sakai, J. Mochida, T.J. Albert, I.M. Shapiro, M.V. Risbud, Hypoxia activates the notch signaling pathway in cells of the intervertebral disc: implications in degenerative disc disease, Arthritis Rheum 63 (2011) 1355–1364.
[72] L. Aker, M. Ghannam, M.A. Alzuabi, F. Jumah, S.M. Alkhdour, S. Mansour, A. Samara, K. Cronk, J. Massengale, J. Holsapple, N. Adeeb, R.J. Oskouian, R.S. Tubbs, Molecular biology and interactions in intervertebral disc development, homeostasis, and degeneration, with emphasis on future therapies: a systematic review, Spine Sch. 1 (2017) 2–20.
[73] S. Mohanty, R. Pinelli, P. Pricop, T.J. Albert, C.L. Dahia, Chondrocyte - like nested cells in the aged intervertebral disc are late - stage nucleus pulposus cells, Aging Cell (2019) 1–5, doi:10.1111/acel.13006.
[74] M. Nagae, T. Ikeda, Y. Mikami, H. Hase, H. Ozawa, K.I. Matsuda, H. Sakamoto, Y. Tabata, M. Kawata, T. Kubo, Intervertebral disc regeneration using platelet-rich plasma and biodegradable gelatin hydrogel microspheres, Tissue Eng. 13 (2007) 147–158.
[75] A.J. Fields, E.C. Liebenberg, J.C. Lotz, Innervation of pathologies in the lumbar vertebral end plate and intervertebral disc, Spine J. 14 (2014) 513–521.